Chapter 2
Analytical Models

This chapter presents the development of the analytical model of the antenna velocity loop. The analytical model includes the antenna structure, its drives, and the velocity loop itself. First, a rigid antenna model is discussed. Next, the modal model of a flexible antenna structure is analyzed based on the finite-element data. The modal model is transferred into the state-space model, in both continuous- and discrete-time. Next, the drive model is derived, and combined into the velocity loop model. Finally, the impact of the drive parameters (gearbox stiffness and motor inertia) on the velocity loop properties is analyzed. It is worth to remind that the analytical model is mainly used in the design stage of the antenna. Due to limited accuracy of the analytical modeling, these models cannot be used in implementation, such as the model-based controllers.

2.1 Rigid Antenna Model

In this section the velocity loop of a rigid-body antenna is analyzed. Such models represents an antenna without flexible deformations in the disturbance frequency band, and are well beyond antenna bandwidth. This is a model of an idealized antenna, with rigid gearboxes and a rigid structure. It might be applicable to small antennas, but in our case it serves as a tool for explaining and deriving basic velocity loop properties in a closed form (while for larger, flexible antennas the analysis is based on Matlab and Simulink simulations). This simple analysis is extended later to illustrate properties of a flexible antenna control system, and for the better insight into more complicated models and their properties.

A rigid antenna in the open loop configuration has torque input and velocity output. The relationship between the torque τ and angular velocity ω follows from the Newton inertia law

$$J\dot{\omega} = \tau \tag{2.1}$$

where J is the antenna inertia. The Laplace transform of the above equation is $Js\omega(s) = \tau(s)$; hence, the antenna transfer function is represented as an integrator

W. Gawronski, *Modeling and Control of Antennas and Telescopes*,
DOI: 10.1007/978-0-387-78793-0_2, © Springer Science+Business Media, LLC 2008

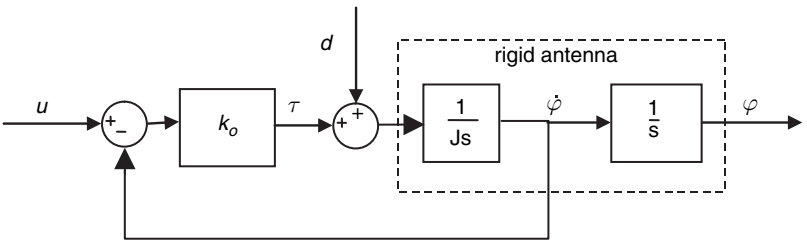

Fig. 2.1 Velocity loop model of a rigid antenna

$$G(s) = \frac{\omega(s)}{\tau(s)} = \frac{1}{Js} \tag{2.2}$$

The velocity loop model of a rigid antenna with a proportional controller is shown in Fig. 2.1. The transfer function of the closed velocity loop system, from the velocity command u to the antenna velocity $\dot{\varphi}$, is as follows:

$$G_{rl}(s) = \frac{\dot{\varphi}(s)}{u(s)} = \frac{k_o G(s)}{1 + k_o G(s)} = \frac{1}{1 + Ts} \tag{2.3}$$

where $T = J/k_o$. The bandwidth of the velocity loop system is equal to $B = 1/T = k_o/J$ rad/s. The gain, k_o, is tuned to obtain the required bandwidth of the system. For example, if the required bandwidth is $B = 20$ rad/s, and the inertia is $J = 1$ Nms^2/rad, then $k_o = 20$ Nms.

2.2 Structural Model

The structural model is typically derived from the finite-element model. It is not the finite-element model per se, but its by-product, the modal model. Note that the modal model includes the rigid-body mode (antenna-free rotation). For the controller tuning purposes the modal model is represented in state-space form, which it is finally given in the discrete-time representation.

2.2.1 Finite-Element Model

The analytical model of an antenna is obtained from its finite-element model. The finite element model of a 34-m antenna is shown in Fig. 2.2. It consists of hundreds of nodes and elements, and thousands of degrees of freedom. The model is characterized by the mass, stiffness, and damping matrices, and by the sensors and actuator locations.

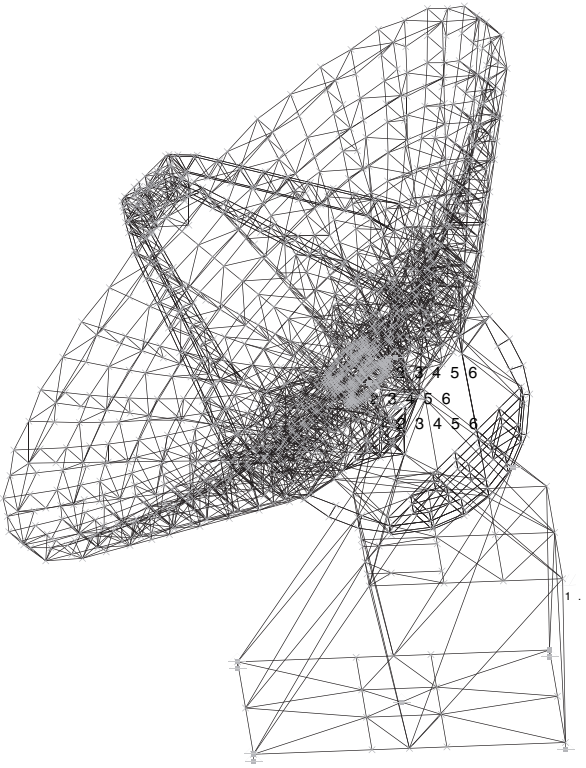

Fig. 2.2 The finite-element model of the 34-m antenna

Let N be a number of degrees of freedom of the finite-element model, with antenna displacement and velocity at the encoder location as the output and force at the motor pinion attachment as the input. Antenna structure is represented by the following second-order matrix differential equation:

$$\begin{aligned} M\ddot{q} + D\dot{q} + Kq &= B_o u, \\ y &= C_{oq} q + C_{ov} \dot{q}. \end{aligned} \tag{2.4}$$

In this equation q is the $N \times 1$ nodal displacement vector; $\dot{q}$ is the $N \times 1$ nodal velocity vector; $\ddot{q}$ is the $N \times 1$ nodal acceleration vector; u is the input; y is the output; M is the mass matrix, $N \times N$; D is the damping matrix, $N \times N$; and K is the stiffness matrix, $N \times N$. The input matrix B_o is $N \times 1$, the output displacement matrix C_{oq} is $1 \times N$, and the output velocity matrix C_{ov} is $1 \times N$. The mass matrix is positive definite (all its eigenvalues are positive), and the

stiffness and damping matrices are positive semi-definite (all their eigenvalues are non-negative).

2.2.2 Modal Model

Modal models of antennas are expressed in modal coordinates. Because these coordinates are independent, they simplify the analysis. The modal model is obtained by transforming equation (2.4) using a modal matrix; see [2].

Consider free vibrations of an antenna structure without damping, and without external excitation, that is, $u = 0$ and $D = 0$. The equation of motion (2.4) in this case turns into the following equation:

$$M\ddot{q} + Kq = 0. \tag{2.5}$$

The solution of the above is $q = \phi e^{j\omega t}$; hence, the second derivative of the solution is $\ddot{q} = -\omega^2 \phi e^{j\omega t}$. Introducing q and $\ddot{q}$ into (2.5) gives

$$(K - \omega^2 M)\phi e^{j\omega t} = 0. \tag{2.6}$$

This set of homogeneous equations has a nontrivial solution if the determinant of $K - \omega^2 M$ is zero, that is,

$$\det(K - \omega^2 M) = 0. \tag{2.7}$$

The above determinant equation is satisfied for a set of n values of frequency ω. These frequencies are denoted $\omega_1, \omega_2, ..., \omega_n$, and their number n does not exceed the number of degrees of freedom, i.e., $n \leqslant N$. The frequency ω_i is called the ith natural frequency.

Substituting ω_i into (2.6) yields the corresponding set of vectors $\{\phi_1, \phi_2, ..., \phi_n\}$ that satisfy this equation. The ith vector ϕ_i corresponding to the ith natural frequency is called the ith mode shape. The natural modes are not unique, since they can be arbitrarily scaled. Indeed, if ϕ_i satisfies (2.6), so does $\alpha\phi_i$, where α is an arbitrary scalar.

For a notational convenience define the matrix of natural frequencies

$$\Omega = \begin{bmatrix} \omega_1 & 0 & \cdots & 0 \\ 0 & \omega_2 & \cdots & 0 \\ \cdots & \cdots & \cdots & \cdots \\ 0 & 0 & \cdots & \omega_n \end{bmatrix} \tag{2.8}$$

and the matrix of mode shapes, or modal matrix Φ, of dimensions $N \times n$, which consists of n natural modes of a structure

$$\Phi = \left[\begin{array}{cccc} \phi_1 & \phi_2 & \ldots & \phi_n \end{array} \right] = \left[\begin{array}{cccc} \phi_{11} & \phi_{21} & \cdots & \phi_{n1} \\ \phi_{12} & \phi_{22} & \cdots & \phi_{n2} \\ \cdots & \cdots & \cdots & \cdots \\ \phi_{1k} & \phi_{2k} & \cdots & \phi_{nk} \\ \cdots & \cdots & \cdots & \cdots \\ \phi_{1n_d} & \phi_{2n_d} & \cdots & \phi_{nn_d} \end{array} \right], \tag{2.9}$$

where ϕ_{ij} is the jth displacement of the ith mode, that is,

$$\phi_i = \left\{ \begin{array}{c} \phi_{i1} \\ \phi_{i2} \\ \vdots \\ \phi_{in} \end{array} \right\}. \tag{2.10}$$

The modal matrix Φ has an interesting property: it diagonalizes mass and stiffness matrices M and K,

$$M_m = \Phi^T M \Phi, \qquad K_m = \Phi^T K \Phi. \tag{2.11}$$

The obtained diagonal matrices are called modal mass matrix (M_m) and modal stiffness matrix (K_m), respectively. The same transformation, applied to the damping matrix

$$D_m = \Phi^T D \Phi, \tag{2.12}$$

gives the modal damping matrix D_m, which is a diagonal if it is, for example, proportional to the stiffness matrix.

In order to obtain the modal model a new variable, q_m, is introduced. It is called modal displacement, and satisfies the following equation:

$$q = \Phi q_m. \tag{2.13}$$

Equation (2.13) is introduced to (2.4), and the latter additionally left-multiplied by Φ^T, obtaining

$$\begin{aligned} &M_m \ddot{q}_m + D_m \dot{q}_m + K_m q_m = \Phi^T B_o u, \\ &y = C_{oq} \Phi q_m + C_{ov} \Phi \dot{q}_m. \end{aligned}$$

using (2.11), and (2.12) notations. Next, the left multiplication of the latter equation by M_m^{-1}, which gives

$$\begin{aligned} &\ddot{q}_m + 2\mathrm{Z}\Omega\dot{q}_m + \Omega^2 q_m = B_m u, \\ &y = C_{mq} q_m + C_{mv}\dot{q}_m. \end{aligned} \tag{2.14}$$

In (2.14) Ω is a diagonal matrix of natural frequencies, defined before, and Z is the modal damping matrix. It is a diagonal matrix of modal damping,

$$\mathrm{Z} = \begin{bmatrix} \zeta_1 & 0 & \cdots & 0 \\ 0 & \zeta_2 & \cdots & 0 \\ \cdots & \cdots & \cdots & \cdots \\ 0 & 0 & \cdots & \zeta_n \end{bmatrix}. \tag{2.15}$$

where ζ_i is the damping of the ith mode. This matrix is obtained using the following relationship $M_m^{-1} D_m = 2\mathrm{Z}\Omega$, thus,

$$\mathrm{Z} = 0.5 M_m^{-1} D_m \Omega^{-1} = 0.5 M_m^{-\frac{1}{2}} K_m^{-\frac{1}{2}} D_m. \tag{2.16}$$

The modal input matrix B_m in (2.14) is as follows

$$B_m = M_m^{-1} \Phi^T B_o. \tag{2.17}$$

Finally, in (2.14) the following notations is used for the modal displacement and velocity matrices:

$$C_{mq} = C_{oq}\Phi, \tag{2.18}$$

$$C_{mv} = C_{ov}\Phi. \tag{2.19}$$

Note that (2.14) (a modal representation of a structure) is a set of uncoupled equations. Indeed, due to the diagonality of Ω and Z, this set of equations can be written, equivalently, as

$$\begin{aligned} &\ddot{q}_{mi} + 2\zeta_i \omega_i \dot{q}_{mi} + \omega_i^2 q_{mi} = b_{mi} u \\ &y_i = c_{mqi} q_{mi} + c_{mvi}\dot{q}_{mi}, \qquad i = 1, \ldots, n, \\ &y = \sum_{i=1}^{n} y_i, \end{aligned} \tag{2.20}$$

where b_{mi} is the ith row of B_m and c_{mqi}, c_{mvi} are the ith columns of C_{mq} and C_{mv}, respectively. In the above equations y_i is the system output due to the ith mode dynamics. Note that the structural response y is a sum of modal responses y_i, which is a key property used to derive structural properties in modal coordinates.

Theoretically the determination of the input and output matrices as in (2.17), (2.18), and (2.19) requires large matrix Φ (of size: number of degrees of freedom

by number of modes). In fact, one needs only one row of it for each input/output matrix. Indeed, the input matrix B_o is all zero, except the location of the actuator (pinion) to the structure. The same, the output matrix C_{mq} is all zero, except the location of the sensor (encoder) to the structure. Let the location of the sensor is at the kth degree of freedom of the finite-element model. The modal matrix is as in (2.9). Because C_{mq} is all zero but the kth entry, therefore

$$C_{mq} = C_{oq}\Phi = \begin{bmatrix} 0\ 0\ \ldots\ 1\ \ldots\ 0 \end{bmatrix} \begin{bmatrix} \phi_{11} & \phi_{21} & \ldots & \phi_{n1} \\ \phi_{12} & \phi_{22} & \ldots & \phi_{n2} \\ \ldots & \ldots & \ldots & \ldots \\ \phi_{1k} & \phi_{2k} & \ldots & \phi_{nk} \\ \ldots & \ldots & \ldots & \ldots \\ \phi_{1n_d} & \phi_{2n_d} & \ldots & \phi_{nn_d} \end{bmatrix} = \begin{bmatrix} \phi_{1k}\ \phi_{2k}\ \ldots\ \phi_{nk} \end{bmatrix} \tag{2.21}$$

that is, C_{mq} consists of modal displacement at the encoder location. Similarly, if the actuator (pinion) is located at the kth degree of freedom, the corresponding input matrix is

$$B_{mq} = \begin{bmatrix} \phi_{1k}/m_{m1} \\ \phi_{2k}/m_{m2} \\ \cdots \\ \phi_{nk}/m_{mn} \end{bmatrix} \tag{2.22}$$

where $m_{mi}$is the ith modal mass. Thus, B_{mq} consists of modal displacement at the actuator (pinion) location scaled by the modal masses.

In summary, from comparatively few parameters of the finite-element model, such as natural frequencies, modal masses, modal damping, and modal displacements at the actuator and sensor locations one creates the antenna structural model in equation (2.14). Note that this structural dynamics model of an antenna is much simpler than its static finite-element model.

As an example, determine the first four natural modes and frequencies of the antenna presented in Fig. 2.2. The modes are shown in Fig. 2.3. For the first mode the natural frequency is $\omega_1 = 13.2$rad/s (2.10 Hz), for the second mode the natural frequency is $\omega_2 = 18.1$ rad/s (2.88 Hz), for the third mode the natural frequency is $\omega_3 = 18.8$ rad/s (2.99 Hz), and for the fourth mode the natural frequency is $\omega_4 = 24.3$ rad/s (3.87 Hz).

2.2.3 State-Space Model

State-space representation is the standard representation of the control system models. Thus, the antenna structure needs to be represented in this form, to allow the use of control system software such as Matlab or Simulink. The modal state-space

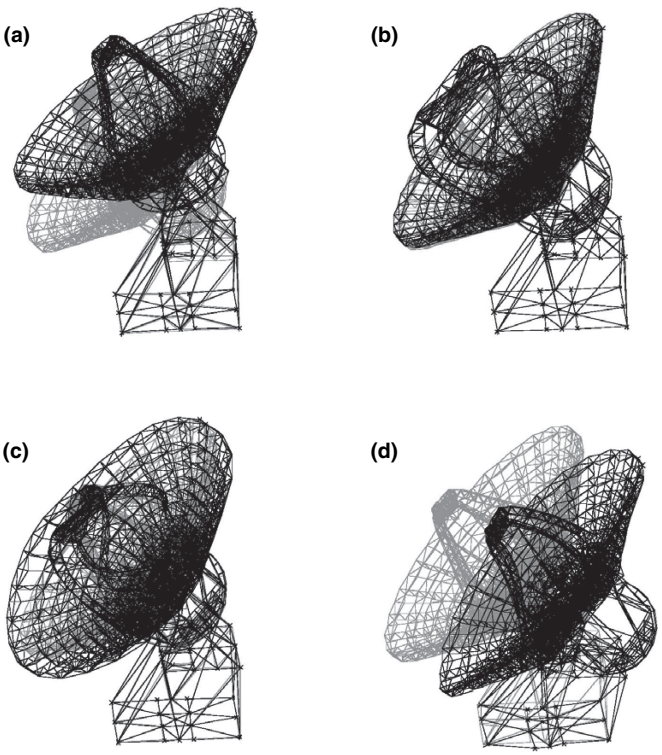

Fig. 2.3 Antenna modes: (**a**) First mode (of natural frequency 2.10 Hz); (**b**) second mode (of natural frequency 2.87 Hz); (**c**) third mode (of natural frequency 2.99 Hz); and (**d**) fourth mode (of natural frequency 3.87 Hz). For each mode the nodal displacements are sinusoidal, have the same frequency, and the displacements are shown at their extreme values. Gray color denotes undeformed state

representation of the antenna structure is a triple (A_m, B_m, C_m) characterized by the block-diagonal state matrix, A_m; see [2]

$$A_m = \mathrm{diag}(A_{mi}) = \left[\begin{array}{cc:cc:ccc:cc} \times & \times & 0 & 0 & \cdots & \cdots & 0 & 0 \\ \times & \times & 0 & 0 & \cdots & \cdots & 0 & 0 \\ \hdashline 0 & 0 & \times & \times & \cdots & \cdots & 0 & 0 \\ 0 & 0 & \times & \times & \cdots & \cdots & 0 & 0 \\ \hdashline \cdots & \cdots & \cdots & \cdots & \cdots & \cdots & \cdots & \cdots \\ \cdots & \cdots & \cdots & \cdots & \cdots & \cdots & \cdots & \cdots \\ \hdashline 0 & 0 & 0 & 0 & \cdots & \cdots & \times & \times \\ 0 & 0 & 0 & 0 & \cdots & \cdots & \times & \times \end{array}\right], \quad i = 1, 2, \ldots, n, \tag{2.23}$$

where A_{mi} are 2×2 blocks (their nonzero elements are marked with $\times$), and the modal input and output matrices are divided, correspondingly,

$$B_m = \begin{bmatrix} B_{m1} \\ B_{m2} \\ \vdots \\ B_{mn} \end{bmatrix}, \qquad C_m = \begin{bmatrix} C_{m1} & C_{m2} & \cdots & C_{mn} \end{bmatrix}, \tag{2.24}$$

The blocks A_{mi}, B_{mi}, and C_{mi} are as follows:

$$A_{mi} = \begin{bmatrix} 0 & \omega_i \\ -\omega_i & -2\zeta_i\omega_i \end{bmatrix}, \qquad B_{mi} = \begin{bmatrix} 0 \\ b_{mi} \end{bmatrix}, \qquad C_{mi} = \begin{bmatrix} \frac{c_{mqi}}{\omega_i} & c_{mvi} \end{bmatrix}; \tag{2.25}$$

The state x of the modal representation consists of n independent components, x_i, that represent a state of each mode

$$x = \begin{Bmatrix} x_1 \\ x_2 \\ \vdots \\ x_n \end{Bmatrix}, \tag{2.26}$$

The ith state component is as follows:

$$x_i = \begin{Bmatrix} \omega_i q_{mi} \\ \dot{q}_{mi} \end{Bmatrix}, \tag{2.27}$$

The ith component, or mode, has the state-space representation (A_{mi}, B_{mi}, C_{mi}) independently obtained from the state equations

$$\begin{aligned} \dot{x}_i &= A_{mi}x_i + B_{mi}u, \\ y_i &= C_{mi}x_i, \\ y &= \sum_{i=1}^{n} y_i. \end{aligned} \tag{2.28}$$

This decomposition is justified by the block-diagonal form of the matrix A_m,

The poles of a structure are the zeros of the characteristic equations . The equation $s^2 + 2\zeta_i\omega_i s + \omega_i^2 = 0$ is the characteristic equation of the ith mode. For small damping the poles are complex conjugate, and in the following form:

$$s_{1,2} = -\zeta_i\omega_i \pm j\omega_i\sqrt{1-\zeta_i^2}. \tag{2.29}$$

The plot of the poles is shown in Fig. 2.4, which shows how the location of a pole relates to the natural frequency and modal damping.

2.2.4 Models with Rigid Body Modes

Antenna structure is unrestrained—it can free rotate with respect to azimuth and elevation axes. Modal analysis for such structures shows that they have zero natural frequency, and that the corresponding natural mode shows structural displacements

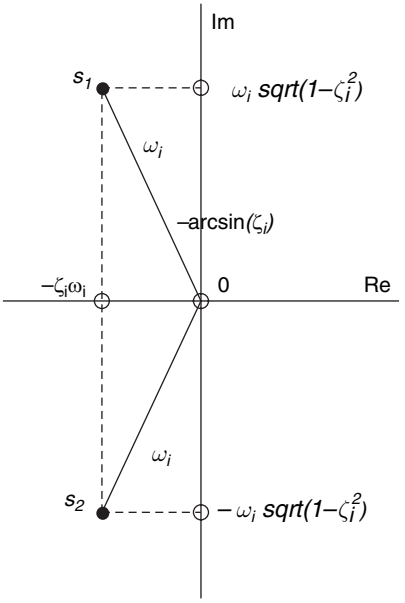

Fig. 2.4 Pole location of the *i*th mode of a lightly damped structure: It is a complex pair with the real part proportional to the *i*th modal damping; the imaginary part approximately equal to the *i*th natural frequency; and the radius is the exact natural frequency

but no flexible deformations. A mode without flexible deformations is called a rigid-body mode. Corresponding zero frequency implies that the zero frequency harmonic excitation (which is a constant force or torque) causes rigid-body movement of the structure. Structural analysts sometimes ignore this mode, as there is no deformation involved. However, it is of crucial importance for a control engineer, because this mode is the one that allows a controller to move a structure and track a command.

The rigid-body modes are obtained by solving the same eigenvalue problem as presented for the standard models. Because the natural frequency is zero, the modal equation becomes $\det(K) = 0$, that is, the stiffness matrix becomes singular. The corresponding rigid-body mode ϕ_{rb} is the one that satisfies the equation

$$K\phi_{rb} = 0. \tag{2.30}$$

The modal equations for the rigid-body modes follow from (2.20) by assuming $\omega_i = 0$, that is,

$$\begin{aligned} \ddot{q}_{mi} &= b_{mi}u, \\ y_i &= c_{mqi}q_{mi} + c_{mvi}\dot{q}_{mi}, \\ y &= \sum_{i=1}^{n} y_i. \end{aligned} \tag{2.31}$$

The state-space modal model for a rigid-body mode is as follows,

$$A_{mi} = \begin{bmatrix} 0 & 1 \\ 0 & 0 \end{bmatrix}, \qquad B_{mi} = \begin{bmatrix} 0 \\ b_{mi} \end{bmatrix}, \qquad C_{mi} = \begin{bmatrix} c_{mqi} & c_{mvi} \end{bmatrix}, \tag{2.32}$$

For the experienced engineer the rigid-body frequency and mode are not difficult to determine: rigid-body frequency is always zero, and rigid-body mode can be predicted as a structural movement without deformation. The importance of distinguishing it from "regular" modes is the fact that they make a system unstable, and thus a system that requires special attention.

The Deep Space Network antenna has two rigid-body modes: rigid-body rotation with respect to the azimuth (vertical) axis, and rigid-body rotation with respect to the elevation (horizontal) axis. Figure 2.5 shows the azimuth rigid-body mode. Figure 2.5(a) presents the initial position from the top view; Fig. 2.5(b) presents the modal displacement (rigid-body rotation with respect to the azimuth axis) from the top view,

2.2.5 Discrete-Time Model

For the antenna performance simulations and for the controller tuning purposes the discrete-time models are required. The discrete time model is obtained from a continuous-time state-space representation (A,B,C). Because the discrete-time sequences of this model are sampled continuous-time signals, that is,

$$x_k = x(k\Delta t), \qquad u_k = u(k\Delta t), \text{ and } y_k = y(k\Delta t), \tag{2.33}$$

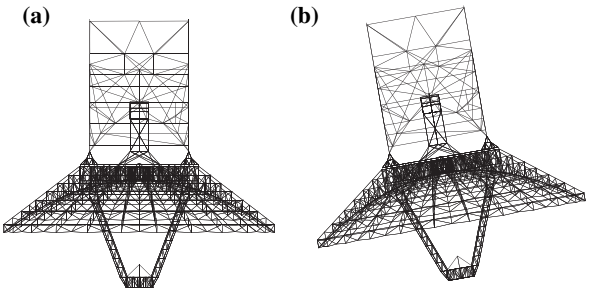

Fig. 2.5 Antenna in neutral position (**a**), and the azimuth rigid-body mode (**b**), where no flexible deformations are observed

for $k = 1, 2, 3 \ldots$, thus the corresponding discrete-time representation for the sampling time Δt is (A_d, B_d, C_d, D_d), where

$$A_d = e^{A\Delta t}, \qquad B_d = \int_0^{\Delta t} e^{A\tau} B d\tau, \qquad C_d = C, \tag{2.34}$$

and the corresponding state-space equations are

$$\begin{aligned} x_{k+1} &= A_d x_k + B_d u_k, \\ y_k &= C x_k. \end{aligned} \tag{2.35}$$

The discretization can be carried out numerically using the *c2d* command of Matlab.

Next, the discrete-time models is presented in modal coordinates. Assume small damping and the sampling rate sufficiently fast, such that the Nyquist sampling theorem is satisfied (i.e., $\omega_i \Delta t \leqslant \pi$ for all i), see, for example, [1, p. 111], then the state matrix in modal coordinates A_{dm} is block-diagonal,

$$A_{dm} = \text{diag}(A_{dmi}), \qquad i = 1, \ldots, n. \tag{2.36}$$

The 2×2 blocks A_{dmi} are in the form (see [4]),

$$A_{dmi} = e^{-\zeta_i \omega_i \Delta t} \begin{bmatrix} \cos(\omega_i \Delta t) & -\sin(\omega_i \Delta t) \\ \sin(\omega_i \Delta t) & \cos(\omega_i \Delta t) \end{bmatrix}, \tag{2.37}$$

where ω_i and ζ_i are the ith natural frequency and the ith modal damping, respectively. The modal input matrix B_{dm} consists of 2×1 blocks B_{dmi},

$$B_{dm} = \begin{bmatrix} B_{dm1} \\ B_{dm2} \\ \vdots \\ B_{dmn} \end{bmatrix}, \tag{2.38}$$

where

$$B_{dmi} = S_i B_{mi}, \qquad S_i = \frac{1}{\omega_i} \begin{bmatrix} \sin(\omega_i \Delta t) & -1 + \cos(\omega_i \Delta t) \\ 1 - \cos(\omega_i \Delta t) & \sin(\omega_i \Delta t) \end{bmatrix}, \tag{2.39}$$

and B_{mi} is the continuous-time modal representation. The discrete-time modal matrix C_{dm} is the same as the continuous-time modal matrix C_m.

The poles of the matrix A_{dm} are composed of the poles of matrices A_{dmi}, $I = 1,\ldots, n$. For the ith mode the poles of A_{dmi} are

$$s_{1,2} = e^{-\zeta_i \omega_i \Delta t}(\cos(\omega_i \Delta t) \pm \sin(\omega_i \Delta t)). \tag{2.40}$$

The location of the poles is shown in Fig. 2.6, which is quite different from the continuous-time system, cf., Fig. 2.5. For a stable system they should be inside the unit circle.

The question arises how to choose the sampling time Δt. Note that from the Nyquist criterion the ith natural frequency is recovered if the sampling rate is at least twice the natural frequency in Hz ($f_i = \omega_i / 2\pi$), that is, if

$$\frac{1}{\Delta t} \geqslant 2 f_i$$

or, if

$$\omega_i \Delta t \leqslant \pi \qquad \text{or} \qquad \Delta t \leqslant \frac{\pi}{\omega_i}. \tag{2.41}$$

Considering all modes, the sampling time will be smaller than the smallest π / ω_i,

$$\Delta t \leqslant \frac{\pi}{\max\limits_i(\omega_i)}. \tag{2.42}$$

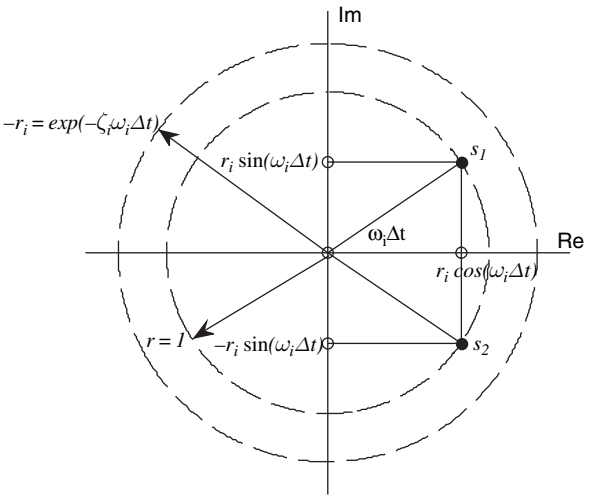

Fig. 2.6 Pole location of the ith mode of a lightly damped structure in discrete time: It is a complex pair with angle proportional to natural frequency and magnitude close to 1

2.3 Drive Model

The drive model consists of motor, reducer, amplifiers, and tachometers.

2.3.1 Motor Model

The motor model is shown in Fig. 2.7. The motor position (θ_m) is controlled by the armature voltage (v_a)

$$v_a = L_a \frac{di_o}{dt} + R_a i_o + k_b \omega_m \tag{2.43}$$

where R_a is motor resistance, L_a is motor inductance, and k_b is the armature constant. The motor torque (T_o) is proportional to the motor current (i_o)

$$T_o = k_m i_o \tag{2.44}$$

where k_m is the motor torque constant. The motor torque, T_o is in equilibrium with the remaining torque acting on the rotor; therefore,

$$T_o = J_m \ddot{\theta}_m + T \tag{2.45}$$

where T is the drive output torque, and J_m is a total inertia of the motor and the brake.

The above equations give the following (after Laplace transform, where s is the Laplace variable)

$$i_o = \frac{v_a - k_b \omega_m}{L_a s + R_a}$$

$$\omega_m = \frac{1}{J_m s}(T_o - T)$$

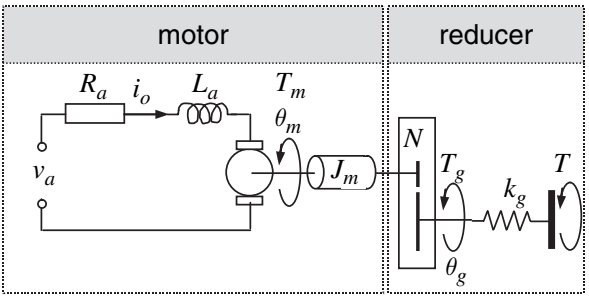

Fig. 2.7 Motor and reducer model

2.3.2 Reducer Model

The reducer model is shown in Fig. 2.7 as well. The torque T at the output of the gearbox can be expressed with the torsional deformation of the gearbox

$$T = k_g(\theta_g - \theta_p) \tag{2.46}$$

θ_p is the angle of rotation of the pinion, k_g is the stiffness of the reducer and drive shaft, N is the reducer gear ratio, θ_g is the angle of rotation of the reducer output shaft

$$\theta_g = \frac{\theta_m}{N} \tag{2.47}$$

2.3.3 Drive Model

Based on the above equations the drive model (e.g., Simulink) is created. Besides motor and reducer, amplifiers are added. A block-diagram of the drive is created; see Fig. 2.8. The parameters of this model are given in Table 2.1.

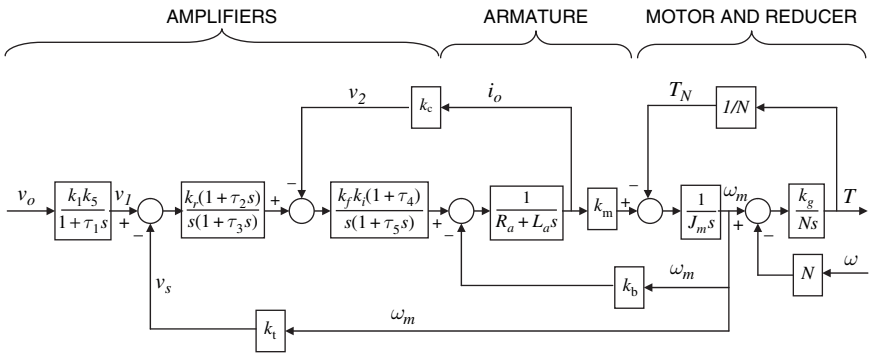

Fig. 2.8 Block diagram of the drive model

Table 2.1 Drive parameters

$k_1 = 716.2$	[V s/rad]	$k_f = 54$ [-]	[-]	$\tau_1 = 0.00637$	[s]
$k_m = 1.787$	[Nm/A]	$k_g = 1.7 \times 10^6$	[Nm/rad]	$\tau_2 = 0.094$	[s]
$k_b = 1.79$	[V s/rad]	$J_m = 0.14$	[Nm/s^2]	$\tau_3 = 0.002$	[s]
$k_s = 0.8$	[-]	$R_a = 0.456$	[Ω]	$\tau_4 = 0.00484$	[s]
$k_t = 0.0384$	[V s/rad]	$L_a = 0.011$	[H]	$\tau_5 = 0.0021$	[s]
$k_r = 80$	[V/s/V]	$N = 354$	[-]	$\tau_6 = 0.7304$	[s]
$k_c = 0.1266$	[V/A]				

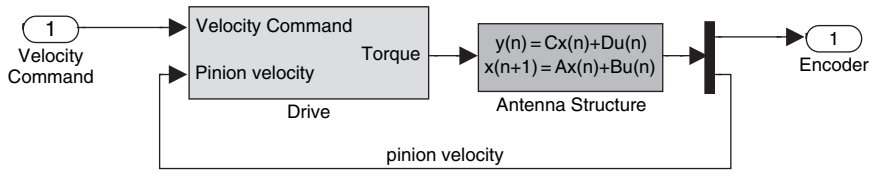

Fig. 2.9 Velocity loop model

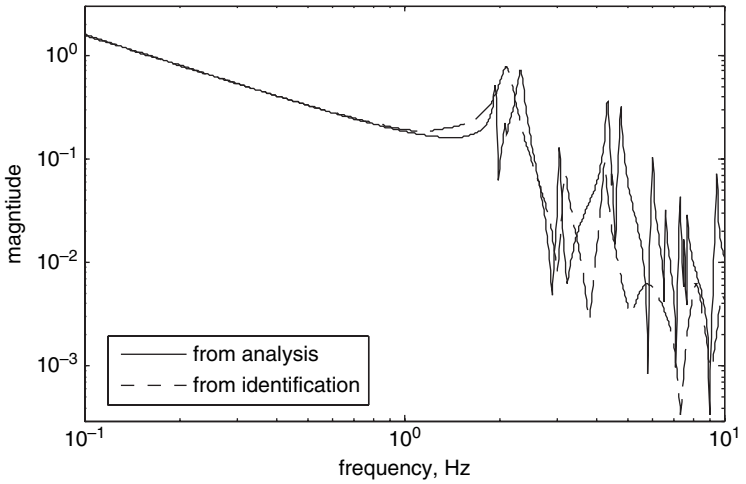

Fig. 2.10 The magnitude of the transfer function of the velocity loop model

2.4 Velocity Loop Model

The Simulink velocity loop model is a combination of the structural and drive models; see Fig. 2.9. The drive torque moves the antenna. The pinion velocity is fed back to the drive to calculate the reducer flexible deformation. The velocity command controls the antenna velocity, and the encoder measures its position.

The magnitude of the velocity loop transfer function is shown in Fig. 2.10, solid line.

2.5 Drive Parameter Study

In this section the effect of the drive inertia and stiffness on the antenna velocity loop properties is investigated. The inertia of the drive includes motor, brake, and gearbox, and the drive stiffness includes gearbox stiffness and shaft stiffness. Because the motor dominates the drive inertia, the motor inertia is investigated, and because gearbox stiffness dominates the drive stiffness, the drive stiffness is investigated.

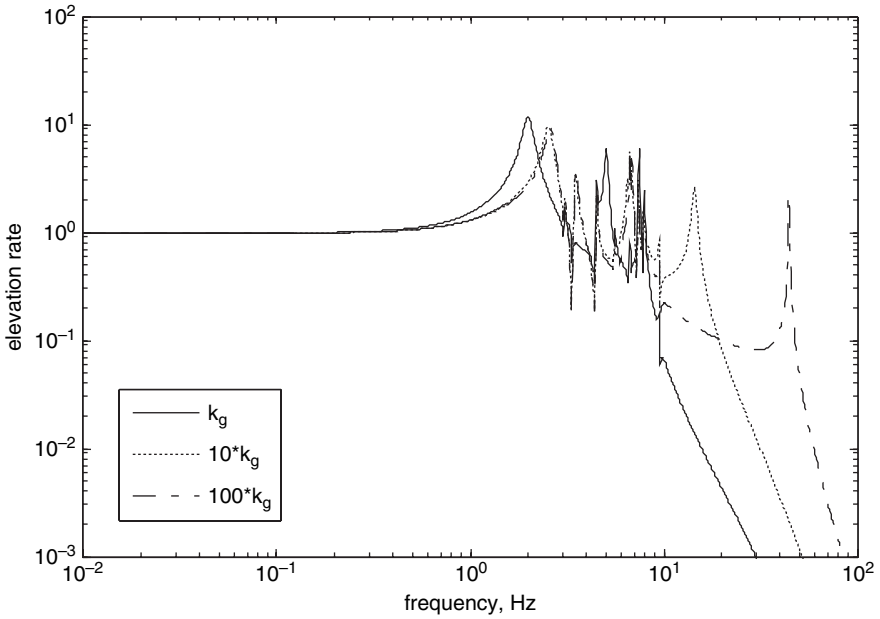

Fig. 2.11 The magnitudes of the transfer function of the velocity loop model for the nominal and increased gearbox stiffness

It is intuitively obvious that a rigid gearbox and a powerful but weightless motor are the best choice for the antenna drive (if they exist). So, what is the smallest allowable gearbox stiffness, or the largest allowable motor inertia? The 34-m antenna velocity loop bandwidth is simulated as a function of motor inertia, and as a function of the gearbox stiffness [3], using the model as in Fig. 2.8 and Fig. 2.9. The nominal motor inertia is 0.14 [Nms^2], and the nominal gearbox stiffness is 1.7×10^6 [N m/rad]; see Table 2.1. The transfer function, from the velocity command to the output velocity for the nominal values, is shown in Fig. 2.11, solid line.

2.5.1 Drive Stiffness Factor

The impact of the gearbox stiffness on the velocity loop properties is simulated, for the nominal gearbox stiffness and for increased stiffness by factors of 10 and 100, respectively. The corresponding transfer functions are shown in Fig. 2.11, dotted (for factor 10) and dot-dashed lines (for factor 100), respectively. One can see that the transfer function bandwidth changed when k_g incresed to $10k_g$. The resonant peak, related to the drive vibration mode shifted to higher frequencies. At the nominal value of the stiffness, the resonant frequency of the drive mode coincided with the structural fundamental frequency. The plots show that the nominal stiffness is

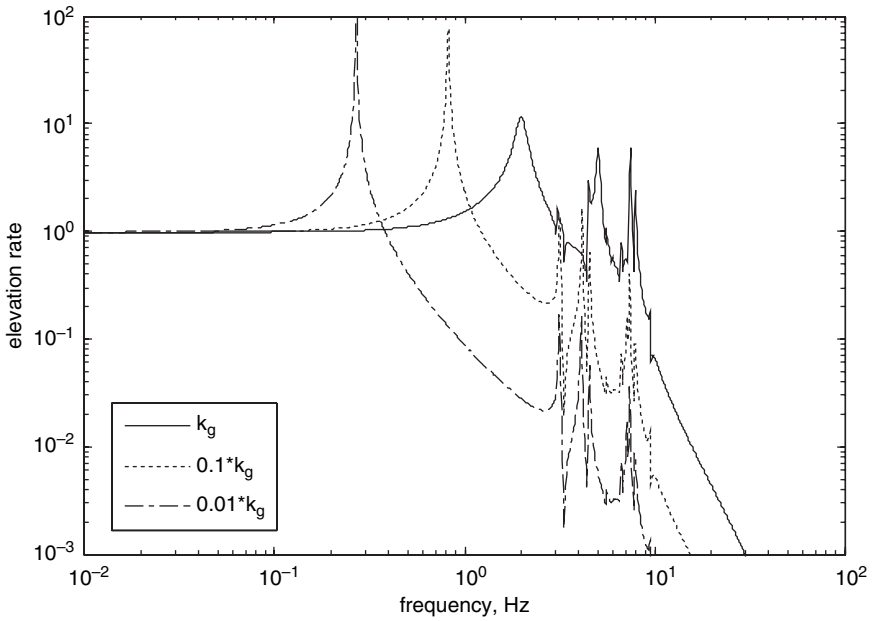

Fig. 2.12 The magnitudes of the transfer function of the velocity loop model for the nominal and decreased gearbox stiffness

slightly too low, because the inreased gearbox stiffness increased the velocity loop bandwidth.

Next, the gearbox stiffness is decreased by factors of 0.1 and 0.01, and the corresponding transfer functions are shown in Fig. 2.12 as dotted and dot-dashed lines, respectively. One can see that the transfer function bandwidth changed significantly. The resonant peak, related to the drive vibration mode is shifted to lower frequencies, impacting the bandwidth. The plots show that the nominal stiffness should not be decreased, because the lower gearbox stiffness impacts the velocity loop bandwidth.

2.5.2 Drive Inertia Factor

Here, the impact of the motor inertia on the velocity loop properties is investigated. The transfer function from the velocity command to the output velocity for the nominal inertia is shown in Fig. 2.13, solid line. First, the motor inertia is decreased by factors 0.1 and 0.01, and the corresponding transfer functions are shown in Fig. 2.13, dotted and dot-dashed lines, respectively. One can see that the transfer function bandwidth changed insignificantly. The resonant peak, related to the drive vibration mode shifted to higher frequencies. The plots show that the nominal inertia

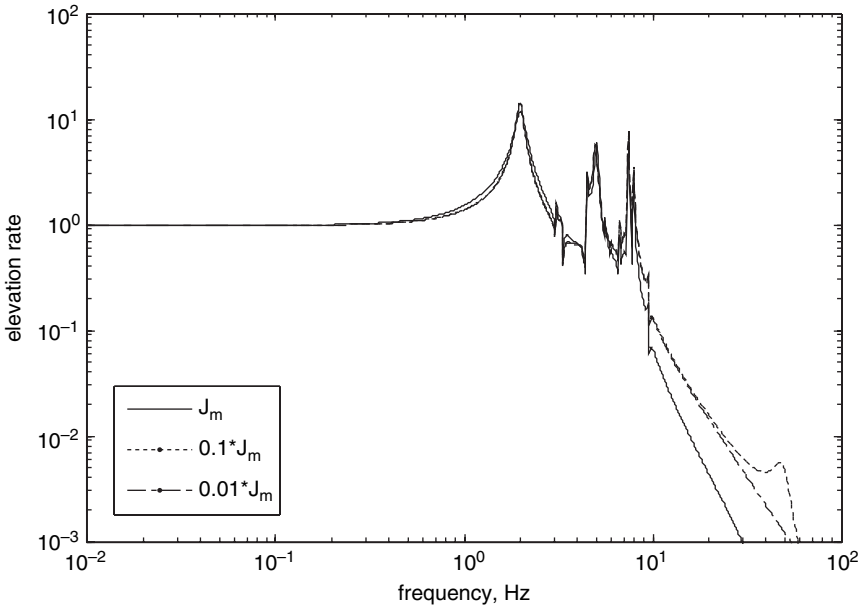

Fig. 2.13 The magnitudes of the transfer function of the velocity loop model for the nominal and decreased motor inertia

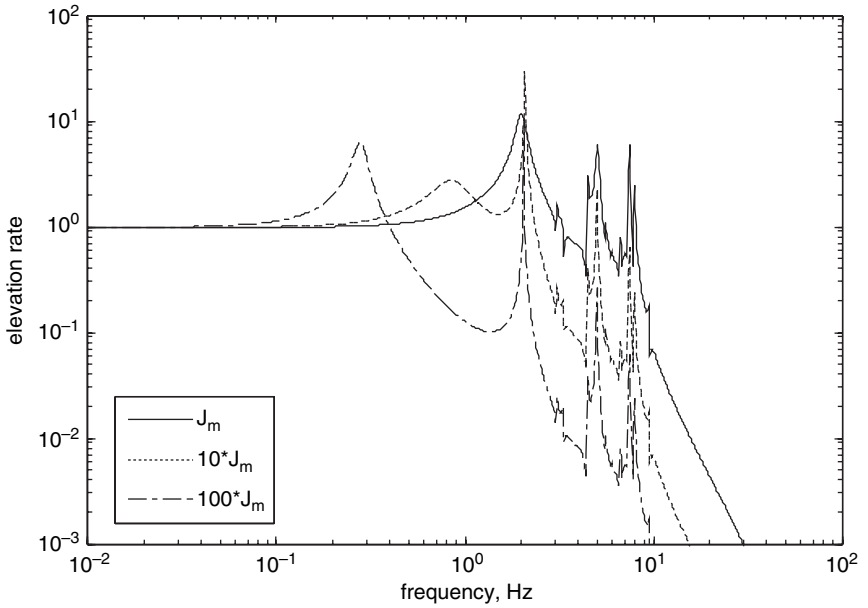

Fig. 2.14 The magnitudes of the transfer function of the velocity loop model for the nominal and increased motor inertia

is sufficient, because the lower motor inertias does not impact the velocity loop bandwidth.

Next, the motor inertia is increased by factors 10 and 100, and the corresponding transfer functions are shown in Fig. 2.14, dotted and dot-dashed lines, respectively. In this case the transfer function bandwidth changed significantly. The resonant peak related to the drive vibration mode is shifted to the lower frequencies, impacting the bandwidth. Note that the antenna fundamental frequency has not been changed. The plots show that the nominal inertia cannot be increased, because it impacts the velocity loop bandwidth.

This simple investigation shows that the gearbox stiffness has its lower limit that should not be violated, because it impacts the velocity loop bandwidth and the closed loop performance. Similarly, the motor inertia has its upper limit. The limit is defined by the antenna fundamental frequency: drive natural frequency should be at least the fundamental frequency of the structure.

References

1. Franklin GF, Powell JD, Workman ML. (1992). *Digital Control of Dynamic Systems.* Addison-Wesley, Reading, MA.
2. Gawronski W. (2004). *Advanced Structural Dynamics and Active Control of Structures.* Springer, New York.
3. Gawronski W, Mellstrom JA. (1992). A Parameter and Configuration Study of the DSS-13 Antenna Drives. *TDA Progress Report*, No.42-110, available at http://ipnpr.jpl.nasa.gov/progress_report/42-110/110S.PDF.
4. Lim KB, Gawronski W. (1996). Hankel Singular Values of Flexible Structures in Discrete Time," *AIAA J. Guidance, Control, and Dynamics*, 19(6):1370–1377.

http://www.springer.com/978-0-387-78792-3

Modeling and Control of Antennas and Telescopes

Gawronski, W.

2008, XVI, 228 p., Hardcover
ISBN: 978-0-387-78792-3